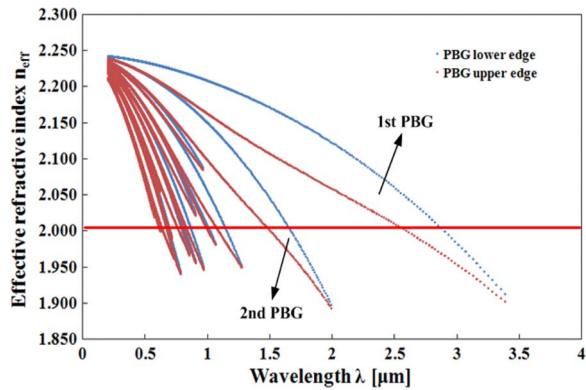


# Numerical Simulation of Dynamic Bandgap Control in All-Solid Chalcogenide–Tellurite Photonic Bandgap Fiber

Volume 5, Number 4, August 2013

Tonglei Cheng  
Yukiko Sakai  
Nur Asyikin  
Weiqing Gao  
Zhongchao Duan  
Dinghuan Deng  
Takenobu Suzuki  
Yasutake Ohishi



---

DOI: 10.1109/JPHOT.2013.2271714  
1943-0655/\$31.00 ©2013 IEEE

# Numerical Simulation of Dynamic Bandgap Control in All-Solid Chalcogenide–Tellurite Photonic Bandgap Fiber

Tonglei Cheng, Yukiko Sakai, Nur Asyikin, Weiqing Gao, Zhongchao Duan,  
Dinghuan Deng, Takenobu Suzuki, and Yasutake Ohishi

Research Center for Advanced Photon Technology, Toyota Technological Institute,  
Nagoya 468-8511, Japan

DOI: 10.1109/JPHOT.2013.2271714  
1943-0655/\$31.00 ©2013 IEEE

Manuscript received May 14, 2013; revised June 7, 2013; accepted June 13, 2013. Date of publication July 4, 2013; date of current version July 10, 2013. This work was supported by MEXT through the Support Program for Forming Strategic Research Infrastructure (2011–2015). Corresponding author: T. Cheng (e-mail: chengtonglei@gmail.com).

**Abstract:** Dynamic bandgap control in all-solid chalcogenide–tellurite photonic bandgap fiber (PBGF) by the refractive index changes due to the optical Kerr effect is numerically simulated in this paper. The core and the cladding with low index are designed by the tellurite glass  $\text{TeO}_2\text{--ZnO}\text{--Li}_2\text{O}\text{--Bi}_2\text{O}_3$ , whereas the high-index rods are designed by the chalcogenide glass GeGaSbS. Because all-solid chalcogenide–tellurite PBGF has higher nonlinear refractive index than the conventional silica PBGF, when the high peak power transmits in this fiber, the refractive index will change due to the optical Kerr effect, and so will the bandgap.

**Index Terms:** Optical Kerr effect, photonic bandgap fiber, the linear refractive index.

## 1. Introduction

In recent years, high speed and broadband communications have been demanded because of the rapid development of the Internet. Conventional step-index optical fibers that have a core and a cladding are used not only in optical communications but also in a wide variety of fields. However, the transmission property of the conventional fibers has reached the theoretical limit, and the transmission capacity is almost saturated. To overcome these limits, a great attention has been attached to multi-core fibers and photonic bandgap fibers (PBGFs) [1]–[4]. In particular, all-solid PBGFs have numerous applications, such as dispersion compensation components, nonlinear optical devices [5], [6], tunable bandpass filters [7], intracavity wavelength selective elements to eliminate amplified spontaneous emission (ASE) [8], [9], etc. All-solid PBGFs are composed of a low index core and the periodic arrangement of high index rods embedded in a low index cladding. Light is confined in the low index core due to the existence of the photonic bandgap (PBG) in the cladding. The guiding regime can also be described analytically by use of the antiresonant reflecting optical waveguide (ARROW) model [10]–[12]. According to this model, the optical properties of all-solid MOFs are governed largely by the thickness and the refractive-index contrast of the first high-index layer rather than by the periodic arrangement of the alternating layers [13]. The propagation wavelength region of all-solid PBGFs corresponds to PBG wavelength region, and light can propagate effectively in the limited wavelength region where PBG exists.

A variety of soft glass, such as tellurite and chalcogenide glasses, possess highly nonlinear refractive indices and practically wide transmission ranges in the mid-IR [14]–[18]. And the soft-glass

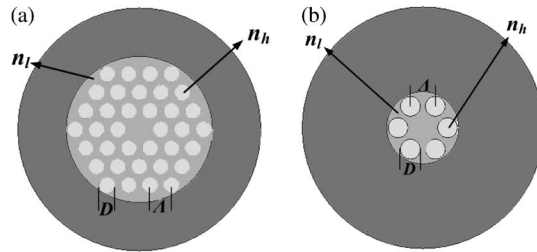


Fig. 1. Structures of all-solid CT-PBGF with (a) three layers and (b) one layer.

fibers are very significant in various applications, such as laser amplifiers, nonlinear effect and optical telecommunications, etc. [19]–[21]. All-solid PBGFs made of a combination of pure and Ge-doped silica have been well studied during the last decade [22], [23]. However, there are only a few studies of all-solid PBGFs which are made of tellurite or chalcogenide glasses. Recently, all-solid tellurite PBGFs have aroused a lot of interest because of their new chapter in nonlinear optics and their potential applications [4], [24]. The optical Kerr effect (OKE) is one of the third-order nonlinear phenomena and it has already been applied to control the phase shift and the dispersion in the optical fiber [25]–[28]. Due to the highly nonlinear refractive indices of the soft-glass fibers, OKE is very obvious. Based on this, PBG of all-solid PBGFs can also be dynamically optical controlled.

In this paper, dynamic optical control of bandgap in all-solid chalcogenide-tellurite PBGF (CT-PBGF) by refractive index changes due to OKE is numerically simulated. The core and the cladding with the low index are designed by the TeO<sub>2</sub>-ZnO-Li<sub>2</sub>O-Bi<sub>2</sub>O<sub>3</sub> (TZLB) glass, while the high-index rods are designed by the GeGaSbS (GGSS) glass. Due to the high nonlinear refractive indices of TZLB and GGSS, OKE is very obvious during the high peak power transmission in all-solid CT-PBGF. Bandgap and the propagation wavelength regions can be controlled dynamically, and this PBGF can offer various propagation wavelength regions and will be utilized to various applications.

## 2. Structure of All-Solid CT-PBGF

During the fabrication of all-solid CT-PBGF, it is important to carefully choose the soft glass, which should have similar thermal and compatible properties to avoid cracking at the interface or disruptions of the core along the fiber axis. Tellurite glass TeO<sub>2</sub>-ZnO-Li<sub>2</sub>O-Bi<sub>2</sub>O<sub>3</sub> (TZLB) was used for the core and the low index cladding, and chalcogenide glass GeGaSbS (GGSS) with high nonlinearity was used for the high index rods. These two glasses have the same thermal expansion coefficient (TEC), which has been proved by our group [29]. The measured softening and drawing temperatures of two glasses are 298 °C and 327 °C, respectively. The microstructured optical fiber (MOF) has already been successfully produced by our group, which confirms that these two glasses can match well during the fabrication process [29]. The structure with three layers shown in Fig. 1(a) was designed, where  $D = 1.647 \mu\text{m}$  is the diameter of GGSS rods, and  $\Lambda$  is the pitch  $D/\Lambda = 0.8$ . The refractive indices of GGSS glass ( $n_h$ ) and TZLB glass ( $n_l$ ) are 2.240 and 2.005, respectively. According to the ARROW model, PBG properties are determined by the refractive index contrast and the thickness of the first high index layer rather than the periodic arrangement and core diameter [11]. So the structure with only one layer of GGSS rods in the cladding can be fabricated, as shown in Fig. 1(b). PBG properties of these two structures are the same.

The refractive index  $n$  which changes by the light intensity is given by

$$n = n_0 + n_2 I_{in} \quad (1)$$

where  $n_0$  is the linear refractive index,  $n_2$  is the nonlinear refractive index, and  $I_{in}$  is the input light intensity. Nonlinearity of an optical fiber is characterized by the nonlinear coefficient  $\gamma$

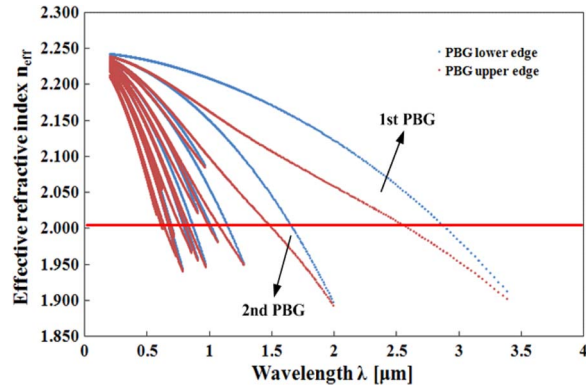


Fig. 2. PBG properties of all-solid CT-PBGF with three layers and one layer.

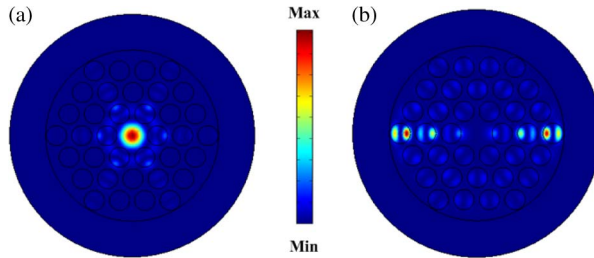


Fig. 3. Optical mode field profiles of three layers all-solid CT-PBGF at (a)  $1.55 \mu\text{m}$  and (b)  $2.10 \mu\text{m}$ .

which is given by

$$\gamma = \frac{n_2 k_0}{A_{\text{eff}}} = \frac{2\pi n_2}{A_{\text{eff}} \lambda_0} \quad (2)$$

where  $k_0$  is the wavenumber in vacuum,  $\lambda_0$  is the wavelength in vacuum and  $A_{\text{eff}}$  is the effective mode area. Larger  $\gamma$  is preferred to enhance the nonlinear effects. When the high peak power launches into all-solid CT-PBGF, the refractive indices of GGSS and TZLB glasses will be changed by OKE from Eq. (1). PBG and propagation properties of the fiber can be controlled by the light intensity. It is expected that PBG properties can be drastically changed by using the control light and high nonlinear refractive index materials, such as tellurite or chalcogenide glasses.

### 3. Numerical Simulation

Simulation of PBG properties of all-solid CT-PBGFs with three layers and one layer has been performed by the plane wave expansion method (PWM) [30], as shown in Fig. 2. We can see that PBG properties of two structures (Fig. 1) are the same. The red line is the core-line and can be expressed by  $n_{\text{eff}} = 2.005$ . Both fiber structures have two main PBGs (1st PBG and 2nd PBG) and the light of wavelength  $1.55 \mu\text{m}$  is confined in the core by the 2nd PBG.

For three layers all-solid CT-PBGF shown in Fig. 1(a), as the light  $1.55 \mu\text{m}$  is within the 2nd PBG, most of the light will be confined in the TZLB core. Some light will extend to the rods, and due to the coupling effect among the modes in the rods, very weak light will be found in the cladding. This feature has already been reported [16], [31]. The optical mode field is calculated by the full vector finite element method, as shown in Fig. 3(a). We can see that most of the power is confined in the core. For the light outside PBG, such as  $2.10 \mu\text{m}$ , it will be confined in the GGSS rods in the

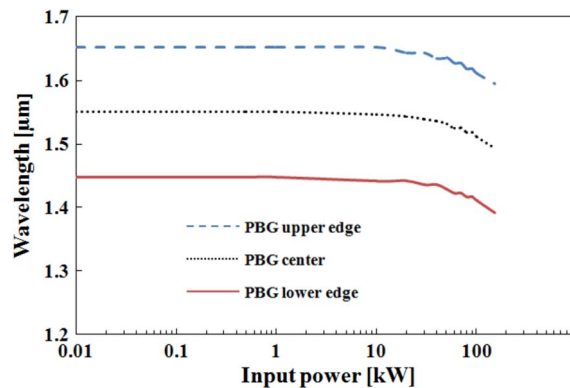


Fig. 4. Second PBG region change by the control light intensity in TZLB core.

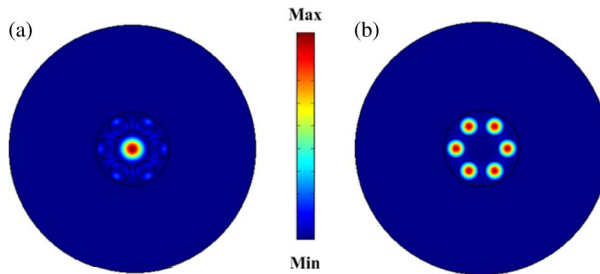


Fig. 5. Optical mode field profiles of one layer all-solid CT-PBGF with only one layer of GGSS at (a)  $1.55 \mu\text{m}$  and (b)  $2.10 \mu\text{m}$ .

cladding, as shown in Fig. 3(b). Due to the coupling effect among the modes in the rods, the light will be lost during the transmission in the CT-PBGF.

If the femtosecond laser at  $1.55 \mu\text{m}$  is used as the pump light, the peak power of several kW level can be easily obtained. The nonlinear refractive index of TZLB core  $n_2 = 2.45 \times 10^{-18} \text{ W/m}^2$  is almost 2 orders magnitude larger than that of a conventional single-mode fiber. So when the high peak power beam transmits in the core by PBG effect, the refractive index of TZLB core changes due to OKE which is very obvious. OKE can be calculated by Eq. (1). Thus bandgap properties of all-solid CT-PBGF can be controlled by the light intensity in TZLB core. Under this condition, a small part of light intensity, which can be neglected, is confined in the inner six GGSS rods. So only OKE in the core are considered and the feasibility of dynamic optical control of the 2nd PBG due to OKE was simulated, as shown in Fig. 4. It can be seen that the 2nd PBG shifts to short wavelengths clearly for more than 10 kW and with the peak power increasing it further shifts to shorter wavelengths. This is because due to OKE, the refractive index of TZLB core increases with the peak power increasing. On the other hand, when the pump light is outside PBG, such as  $\lambda = 2.10 \mu\text{m}$ , it will be lost in the cladding due to the coupling effect, as shown Fig. 3(b). For this case, OKE is very weak and PBG properties of all-solid CT-PBGF will not change by the light intensity.

For one layer all-solid CT-PBGF shown in Fig. 1(b), the optical mode fields at  $\lambda = 1.55 \mu\text{m}$  and  $\lambda = 2.10 \mu\text{m}$  were calculated, as shown in Fig. 5. We can see that when the light is within PBG ( $\lambda = 1.55 \mu\text{m}$ ), most of the light is confined in the core and PBG properties controlled by OKE is the same as Fig. 4. However, when the light is outside PBG ( $\lambda = 2.10 \mu\text{m}$ ), it transmits in the six GGSS rods and is not lost in the cladding. This is because there is no coupling effect between the layers shown in Fig. 3(b), and all-solid CT-PBGF can be considered as a six-core fiber. Fig. 5(b) shows the fundamental in-phase supermode and there are other five high-order supermodes. Only the former

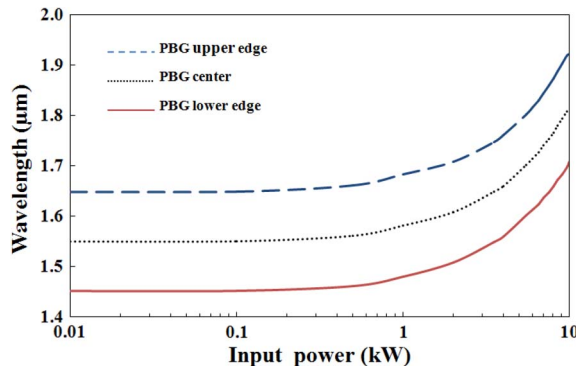


Fig. 6. Second PBG region change by the control light intensity in GGSS rods.

is considered and for one layer all-solid CT-PBGF, the refractive index of GGSS rods will change due to OKE. We further simulated the feasibility of dynamic control of the 2nd PBG in one layer all-solid CT-PBGF, as shown in Fig. 6, where the nonlinear refractive index of GGSS  $n_2 = 1.8 \times 10^{-17} \text{ m}^2/\text{W}$  was used to calculate Eq. (1) [28]. It can be seen that the 2nd PBG shifts to long wavelengths clearly for more than 1 kW. For the pump power of more than 4 kW, the wavelength  $1.55 \mu\text{m}$  is out of PBG region and the light cannot propagate in the core. For the pump power of 10 kW, the 2nd PBG shift is about 265 nm. On the other hand, the width of the 2nd PBG is almost independent of the intensity of the control light. The same trend occurred in other PBGs. According to the above results, it is confirmed that PBG of all-solid CT-PBGF can be controlled dynamically by the light intensity.

#### 4. Summary

Dynamic optical control of bandgap properties in all-solid CT-PBGF by refractive index changes due to OKE is numerically analyzed. When the light is within PBG and confined in TZLB core, PBG will shift to short wavelengths due to OKE with the pump power increasing. When the light is outside PBG, for one layer all-solid CT-PBGF, it is confined in the six GGSS rods and PBG will shift to long wavelengths due to OKE with the pump power increasing. However, for all-solid CT-PBGF with several layers, light will be lost in the cladding and OKE is very weak. Therefore, bandgap and the propagation wavelength regions in all-solid CT-PBGF will be controlled dynamically, thus one fiber would offer various propagation wavelength regions and can be utilized to various applications.

---

#### References

- [1] T. F. S. Büttner, D. D. Hudson, E. C. Mägi, A. C. Bedoya, T. Taunay, and B. J. Eggleton, "Multicore, tapered optical fiber for nonlinear pulse reshaping and saturable absorption," *Opt. Lett.*, vol. 37, no. 13, pp. 2469–2471, Jul. 2012.
- [2] B. Zhu, T. F. Taunay, M. Fishteyn, X. Liu, S. Chandrasekhar, M. Yan, J. M. Fini, E. M. Monberg, and F. V. Dimarcello, "Space-, wavelength-, polarization-division, multiplexed transmission of 56-Tb/s over a 76.8-km seven-core fiber," presented at the Optical Fiber Communication Conf., Los Angeles, CA, USA, Mar. 2011, Paper PDPB7.
- [3] J. C. Knight, J. Broeng, T. A. Birks, and P. S. J. Russell, "Photonic band gap guidance in optical fibers," *Science*, vol. 282, no. 5393, pp. 1476–1478, Nov. 1998.
- [4] T. L. Cheng, Z. C. Duan, M. S. Liao, W. Q. Gao, D. H. Deng, T. Suzuki, and Y. Ohishi, "A simple all-solid tellurite microstructured optical fiber," *Opt. Exp.*, vol. 21, no. 3, pp. 3318–3323, Feb. 2013.
- [5] A. Béroudé, A. Kudlinski, G. Bouwmans, O. Vanvincq, A. Mussot, and Y. Quiquempois, "Control of supercontinuum generation and soliton self-frequency shift in solid-core photonic bandgap fibers," *Opt. Lett.*, vol. 34, no. 20, pp. 3083–3085, Oct. 2009.
- [6] B. Kibler, T. Martynkien, M. Szpulak, C. Finot, J. Fatome, J. Wojcik, W. Urbanczyk, and S. Wabnitz, "Nonlinear femtosecond pulse propagation in an all-solid photonic bandgap fiber," *Opt. Exp.*, vol. 17, no. 12, pp. 10 393–10 398, Jun. 2009.
- [7] M. Chen, A. Shirakawa, X. Fan, K. Ueda, C. B. Olausson, J. K. Lyngs, and J. Broeng, "Single-frequency ytterbium doped photonic bandgap fiber amplifier at 1178 nm," *Opt. Exp.*, vol. 20, no. 19, pp. 21 044–21 052, Sep. 2012.
- [8] A. Wang, A. K. George, and J. C. Knight, "Three-level neodymium fiber laser incorporating photonic bandgap fiber," *Opt. Lett.*, vol. 31, no. 10, pp. 1388–1390, May 2006.

- [9] B. W. Liu, M. L. Hu, X. H. Fang, Y. F. Li, L. Chai, J. Y. Li, W. Chen, and C. Y. Wang, "Tunable bandpass filter with solid-core photonic bandgap fiber and Bragg fiber," *IEEE Photon. Technol. Lett.*, vol. 20, no. 8, pp. 581–583, Apr. 2008.
- [10] M. A. Duguay, Y. Kukubun, T. L. Koch, and L. Pfeiffer, "Antiresonant reflecting optical waveguides in SiO<sub>2</sub>-Si multiplayer structures," *Appl. Phys. Lett.*, vol. 49, no. 1, pp. 13–15, Jul. 1986.
- [11] N. M. Litchinitser, A. K. Abeeluck, C. Headley, and B. J. Eggleton, "Antiresonant reflecting photonic crystal optical waveguide," *Opt. Lett.*, vol. 27, no. 18, pp. 1592–1594, Sep. 2002.
- [12] A. K. Abeeluck, N. M. Litchinitser, C. Headley, and B. J. Eggleton, "Analysis of spectral characteristics of photonic bandgap waveguides," *Opt. Exp.*, vol. 10, no. 23, pp. 1320–1333, Nov. 2002.
- [13] T. P. White, R. C. McPhedran, C. Martijnde Sterke, N. M. Litchinitser, and B. J. Eggleton, "Resonance and scattering in microstructured optical fibers," *Opt. Lett.*, vol. 27, no. 22, pp. 1977–1979, Nov. 2002.
- [14] V. V. Ravi Kanth Kumar, A. K. George, J. C. Knight, and P. J. St. Russell, "Tellurite photonic crystal fiber," *Opt. Exp.*, vol. 11, no. 20, pp. 2641–2645, Oct. 2003.
- [15] M. S. Liao, X. Yan, Z. C. Duan, T. Suzuki, and Y. Ohishi, "Tellurite photonic nanostructured fiber," *J. Lightwave Technol.*, vol. 29, no. 7, pp. 1018–1025, Apr. 2011.
- [16] J. Lousteau, G. Scarpignato, G. Athanasiou, E. Mura, N. Boetti, M. Olivero, T. Benson, and D. Milanese, "Photonic bandgap confinement in an all-solid tellurite glass photonic crystal fiber," *Opt. Lett.*, vol. 37, no. 23, pp. 4922–4924, Dec. 2012.
- [17] A. X. Lin, A. Ryasnyanskiy, and J. Toulouse, "Tunable third-harmonic generation in a solid-core tellurite glass fiber," *Opt. Lett.*, vol. 36, no. 17, pp. 3437–3439, Sep. 2011.
- [18] D. Buccoliero, H. Steffensen, O. Bang, H. Ebendorff-Heidepriem, and T. M. Monro, "Thulium pumped high power supercontinuum in loss-determined optimum lengths of tellurite photonic crystal fiber," *Appl. Phys. Lett.*, vol. 97, no. 6, p. 061106, Aug. 2010.
- [19] I. C. M. Littler, L. B. Fu, E. C. Mägi, D. Pudo, and B. J. Eggleton, "Widely tunable, acousto-optic resonances in Chalcogenide As<sub>2</sub>Se<sub>3</sub> fiber," *Opt. Exp.*, vol. 14, no. 18, pp. 8088–8095, Sep. 2006.
- [20] F. Prudenzano, L. Mescia, L. Allegretti, V. Moizan, V. Nazabal, and F. Smektała, "Theoretical study of cascade laser in erbium-doped chalcogenide glass fibers," *Opt. Mater.*, vol. 33, no. 2, pp. 241–245, Dec. 2010.
- [21] N. Granzow, S. P. Stark, M. A. Schmidt, A. S. Tverjanovich, L. Wondraczek, and P. J. St. Russell, "Supercontinuum generation in chalcogenide silica step-index fibers," *Opt. Exp.*, vol. 19, no. 21, pp. 21 003–21 010, Oct. 2011.
- [22] J. Riishede, J. Lgsgaard, J. Broeng, and A. Bjarklev, "All-silica photonic bandgap fibre with zero dispersion and a large mode area at 730 nm," *J. Opt. Amer.*, vol. 6, no. 7, pp. 667–670, Jul. 2004.
- [23] J. M. Stone, G. J. Pearce, F. Luan, T. A. Birks, J. C. Knight, A. K. George, and D. M. Bird, "An improved photonic bandgap fiber based on an array of rings," *Opt. Exp.*, vol. 14, no. 13, pp. 6291–6296, Jun. 2006.
- [24] T. L. Cheng, M. S. Liao, W. Q. Gao, Z. C. Duan, T. Suzuki, and Y. Ohishi, "A suppression of stimulated Brillouin scattering in all-solid chalcogenide-tellurite photonic bandgap fiber," *Opt. Exp.*, vol. 20, no. 27, pp. 28 846–28 854, Dec. 2012.
- [25] J. M. Dziedzic, R. H. Stolen, and A. Ashkin, "Optical Kerr effect in long fibers," *Appl. Opt.*, vol. 20, no. 8, pp. 1403–1405, Apr. 1981.
- [26] K. Okamoto and E. A. J. Marcatili, "Chromatic dispersion characteristics of fibers with optical Kerr-effect nonlinearity," *J. Light. Technol.*, vol. 7, no. 12, pp. 1988–1994, Dec. 1989.
- [27] C. Breé, A. Demircan, and G. Steinmeyer, "Saturation of the all-optical Kerr effect," *Phys. Rev. Lett.*, vol. 106, no. 18, p. 183 902, May 2011.
- [28] L. Liu, Q. Tian, M. Liao, D. Zhao, G. Qin, Y. Ohishi, and W. Qin, "All-optical control of group velocity dispersion in tellurite photonic crystal fibers," *Opt. Lett.*, vol. 37, no. 24, pp. 5124–5126, Dec. 2012.
- [29] T. Kohoutek, Z. Duan, H. Kawashima, X. Yan, T. Suzuki, M. Matsumoto, T. Misumi, and Y. Ohishi, "Chalcogenide-Tellurite composite microstructured optical fibre," in *Proc. SPIE*, Feb. 2012, p. 82 570D.
- [30] S. Guo and S. Albin, "Simple plane wave implementation for photonic crystal calculations," *Opt. Exp.*, vol. 11, no. 2, pp. 167–175, Jan. 2003.
- [31] A. Bétourné, V. Pureur, G. Bouwmans, Y. Quiquempois, L. Bigot, M. Perrin, and M. Douay, "Solid photonic bandgap fiber assisted by an extra air-clad structure for low-loss operation around 1.5 μm," *Opt. Exp.*, vol. 15, no. 2, pp. 316–324, Jan. 2007.